DECADAL VARIABILITY OF THE PACIFIC SUBTROPICAL CELLS AND EQUATORIAL SEA SURFACE TEMPERATURE

A Thesis
Presented to
The Academic Faculty

by

Carina Saxton Young

In Partial Fulfillment
of the Requirements for the Degree
Master of Sciences in the
School of Earth and Atmospheric Sciences

Georgia Institute of Technology
December 2009

DECADAL VARIABILITY OF THE PACIFIC SUBTROPICAL CELLS AND EQUATORIAL SEA SURFACE TEMPERATURE

Approved by:

Dr. Emanuele Di Lorenzo, Advisor
School of Earth and Atmospheric Sciences
Georgia Institute of Technology

Dr. Annalisa Bracco
School of Earth and Atmospheric Sciences
Georgia Institute of Technology

Dr. Jean Lynch-Stieglitz
School of Earth and Atmospheric Sciences
Georgia Institute of Technology

Date Approved: November 16, 2009

ACKNOWLEDGEMENTS

I would like to thank my advisor, Dr. Emanuele Di Lorenzo, my committee members, Drs. Annalisa Bracco and Jean Lynch-Stieglitz, and my friends and family for their encouragement and assistance.

TABLE OF CONTENTS

LIST OF FIGURES

SUMMARY

This thesis investigates possible dynamical pathways through which variability in the extra-tropical Pacific Ocean influences decadal fluctuations of tropical Pacific sea surface temperatures (SST). Specifically, we examine the hypothesis that low-frequency changes in the Pacific's meridional subtropical cells (STCs), which transport subsurface water masses equatorward from the extra-tropical into the tropical Pacific upwelling system, modulate decadal variations of the equatorial SST. The relationship between the STCs and equatorial Pacific SST anomalies is explored statistically using the monthly hindcast output from the Ocean General Circulation Model (OGCM) for the Earth Simulator (OFES). We find that decadal variability of the subsurface heat transport of the southern branch of the STC is more closely correlated (R = -0.74) with eastern equatorial SST anomalies on timescales longer than 8 years. The northern branch of the STC is overall not well correlated with equatorial SSTa; however, we find that in the period before the 1976 climate shift, the northern cell is more strongly and significantly correlated with equatorial SSTa (R = -0.89, >99%), while the southern cell is not (R = -0.32).

The physical significance of these findings remain unclear and requires isolating mechanisms that could lead to an asymmetry in the role of the northern and southern STC in modulating eastern equatorial SSTa during different states of the Pacific climate. This will be a critical step to attribute physical significance to the statistical changes observed before and after the 1976 climate shift.

CHAPTER I

INTRODUCTION

The synergism between atmospheric and oceanic variability has an enormous impact on physical and biological properties such as temperature, precipitation, and fish populations. On interannual timescales variability is predominantly due to atmospheric forcing (e.g., Delworth, 1996) while on interdecadal timescales the ocean plays the major role via instabilities of the thermohaline circulation (Huck et al., 1999; Colin de Verdière and Huck, 1999; Te Raa and Dijkstra, 2001). On decadal timescales, however, variability is likely due to the dynamics of both the atmosphere and the ocean (Latif and Barnett, 1994). The longer time scales of oceanic processes compared to atmospheric processes means the ocean plays a role in decadal scale variability of the climate.

Long term time series in the Pacific exhibit sudden transitions or regime shifts that typically persist on decadal time scales. An example occurred in the late 1970s when biologists observed drastic changes in the Pacific Ocean's climate and marine ecosystems. This event was due to the "shift" in the ocean-atmosphere system that took place in 1976-77 (e.g. Miller et al, 1994; Nitta and Yamada, 1989; Trenberth and Hurrell, 1994) and sparked the growing interest in Pacific decadal variability.

Decadal variations in the equatorial and midlatitude Pacific can interact via advection along isopycnals, wave propagation, and atmospheric connections (e.g. Gu and Philander, 1997; Schneider et al, 2005). Observational evidence (McPhaden and Zhang, 2002) suggest that another pathway of interaction between the extra-tropics and the tropics is via shallow (0-500 meters) the meridional overturning circulations located between the equator and 10 degrees poleward in both the Atlantic and Pacific Oceans. Such forms of circulation are known as subtropical cells (STCs). Transport variations in the STCs can drive changes in equatorial sea surface temperature (SST) by bringing cool

water to the equatorial upwelling zone from the subtropics (McCreary and Lu, 1994). These changes in tropical SST have immense impact on global climate and ecology (e.g. Trenberth et al., 1998). Here we explore the relationship between low-frequency variability in the STCs and equatorial sea surface temperature anomalies (SSTa) in the Pacific Ocean in relation to the northern and southern subtropical gyres and zonal wind stress.

This thesis is organized as follows. Chapter 1 starts with a brief review on decadal variability, subtropical cells, and subtropical gyres in the Pacific Ocean. Chapter 2 describes the modeling data sets used in this study and methods employed. Chapter 3 contains the results showing the relationship between low-frequency variability in the STCs and equatorial (SSTa). Chapter 4 ends with the summary and conclusions.

1.1 Decadal Variability

In the North Pacific, there are two dominant modes of decadal variability in the atmosphere. One of these is associated with sea level pressure anomalies (SLPa) in the Aleutian Low (e.g. Trenberth and Hurrell, 1994). The Aleutian Low is a semi permanent low pressure center located near the Aleutian Islands in the central North Pacific. It dominates the wind field in the region and represents the first mode of SLP variability in the North Pacific. This low varies from winter to winter in its extent and depth as indicated by the time series of the Aleutian Low Pressure Index (ALPI). The ALPI is a measure of the area of the low pressure region (where SLP $\leq$ 100.5 kPa) and thus is greater when the pressure decreases. Strengthening of the Aleutian Low is associated with a decrease in SST in the central North Pacific. This results from the advection of cool, dry air from the north, an increase in the westerly winds, and an increase of equatorward advection of temperature by Ekman currents. Conversely, the eastern Pacific experiences anomalously warm SST as the strengthened Aleutian Low enhances poleward winds (Schneider and Cornuelle, 2005).

The oceanic expression of the Aleutian Low is the Pacific Decadal Oscillation (PDO) (Mantua et al. 1997). The PDO is characterized as the dominant mode of SSTa in the North Pacific poleward of 20°N (Mantua et al., 1997). It is also highly correlated with the dominant mode of sea surface height anomalies (SSHa) in the region (Chhak et al., 2009). The temporal evolution of the PDO index can be reconstructed with a simple auto-regressive model of order 1 (AR-1) forced by atmospheric variability associated with the Aleutian Low (Schneider and Cornuelle, 2005; Chhak et al., 2009). The PDO has a spatial structure fluctuating between warm and cool phases. The warm phase is associated with cool SSTa over the western and central Pacific with warm SSTa along the west coast of North America and in the tropics. This phase tends to see an increase in ocean biological productivity off the coast of Alaska and a decrease off the western coast of North America (Hare et al, 1999). During the cool phase, the western and central Pacific experience warm SSTa while the eastern Pacific and tropics experience cool SSTa. Productivity during this phase is the reverse of the warm phase, decreasing off the coast of Alaska and increasing off the western coast of North America (Hare et al, 1999).

The second dominant mode of decadal variability in the atmosphere in the North Pacific is associated with the North Pacific Oscillation (NPO) (Walker and Bliss, 1932). It was noted that "pressure variations at Hawaii were opposed to those over Alaska and Alberta, and that high pressure in Alaska meant a more southerly track of 'lows' and more rain in parts of the United States and liability to cold weather east of the Rocky Mountains " (Walker and Bliss, 1932, p. 57). Its spatial pattern consists of a dipole structure characterized by high pressure over Hawaii and low pressure over the Gulf of Alaska. Walker and Bliss (1932) developed the NPO index using monthly mean SLP and surface air temperature (SAT). The NPO emerges as the second mode of SLPa in the North Pacific (Linkin and Nigam, 2008; Walker and Bliss, 1932; Rogers, 1981).

The NPO also has an oceanic expression, termed the North Pacific Gyre Oscillation (NPGO) (Di Lorenzo et al., 2008). Fluctuations in the NPGO correspond to

changes in the strength of the eastern and central branches of the subpolar and subtropical gyres exhibiting a dipole structure (Di Lorenzo et al., 2008). Its pattern emerges as the second dominant mode of SSH variability in the Northeast Pacific. The NPGO is highly correlated with decadal fluctuations in salinity, nutrients, chlorophyll, and many zooplankton species that are not fully explained using the PDO index (Di Lorenzo et al., 2008).

In the tropics, climate variability can be described by two well-known indices, the Southern Oscillation Index (SOI) and the Niño 3.4 index. The Southern Oscillation was first described by Walker in 1928 as a seesaw in the surface pressure between the South Pacific and the Indian Ocean. Its effect on the climate in the tropical Pacific is extensive, including fluctuations in rainfall, SST, and intensity of the trade winds (e.g. Horel and Wallace, 1981; van Loon and Madden, 1981; Philander, 1983). Originally, El Niño was the local name for seasonal warm currents flowing south along the coast of Peru occurring within a few months of Christmas. It was thought to be a local phenomenon due to a lessening or cessation of coastal upwelling along Peru resulting from changes in alongshore winds; however, direct observational evidence showed that the winds did not change in direction or magnitude and that upwelling was occurring. El Niño events are now considered to be perturbations of the ocean-atmosphere system and are defined as excessive SSTa in the tropical Pacific Ocean (Wyrtki, 1975). The east-west redistribution of warm SST involved in the Southern Oscillation causes the thermocline to deepen in the eastern tropical Pacific while shoaling in the west during an El Niño event. Together, El Niño and the Southern Oscillation are components of a single large-scale, ocean-atmosphere interaction known as El Niño/Southern Oscillation (ENSO).

Atmospheric teleconnections between the tropics and the extratropics during ENSO events have been shown to drive an important fraction of the Aleutian Low variability. This variability is then integrated by the ocean into low-frequency variations in the PDO. Additionally, though ENSO events dominate interannual variations in

tropical SSTa, occurring every two to seven years, low-frequency variability in the tropics have been documented (e.g. Trenberth and Hurrell, 1994; Graham, 1994; Wang, 1995; Kleeman et al, 1996; Latif et al., 1997).

Recently, interest has been growing in determining the origin of decadal modulations in the tropics. Many observational and modeling studies have found links between equatorial SSTa with those in the midlatitudes (e.g. Pierce et al., 2000; Deser et al., 2004). Pierce et al. (2000) found significant correlations between low-frequency SSTa in the central North Pacific and the equatorial region. Di Lorenzo et al. (2009) showed that the dynamics of the PDO and NPGO on decadal timescales are physically linked to each other and to tropical variability via ENSO. The mature phase of ENSO and its atmospheric teleconnections to the Aleutian Low are captured by the first dominant mode of ocean/atmosphere co-variability in the Pacific Ocean, while the NPGO/NPO tropical expression (leading the ENSO mode by ~8-12 months) is captured by the second mode (Di Lorenzo et al., 2009).

1.2 Subtropical Cells

Physical mechanisms that link the equatorial and midlatitude Pacific Ocean on decadal timescales include adjustment of ocean circulation via Rossby wave propagation in the midlatitudes (Latif and Barnett, 1996) and Kelvin wave propagation (Enfield and Allen, 1980; Lysne et al., 1997). This connection results from the westward propagation of midlatitude thermal anomalies as long Rossby waves moving toward the western boundary. These waves reach the coast and propagate equatorward as coastal Kelvin waves (Lysne et al., 1997). Atmospheric processes provide another link via the near-simultaneous communication between the regions affected by atmospheric variability. Midlatitude SSTa can drive changes in the trade winds, altering the slope of the tropical thermocline and, therefore, the decadal variability of ENSO (Pierce et al., 2000).

Another mechanism by which direct interaction between the tropics and extra-tropics occurs is by the STCs. The subtropical cells are defined as the meridional transport of water via advection along isopycnals occurring in both the Pacific and Atlantic Oceans (McCreary and Lu, 1994). The thermocline is composed of ventilated layers that are exposed to the ocean surface (Luyten et al., 1983). These "vents" allow the injection of surface water properties (such as temperature and salinity) onto the isopycnals, where they are subducted and can propagate (Stommel, 1979). In the STCs, water is subducted into the thermocline in the subtropics of both hemispheres. The water masses are ventilated in the outcrop regions and are exposed to diabatic exchanges with the atmosphere. They are then subducted and advected to the tropical region via western boundary undercurrents or via meridional pathways in the interior along isopycnals in the main thermocline. Upon reaching the equatorial region, the water upwells into the surface layers and flows poleward out of the tropics (McCreary and Lu, 1994).

The STCs can lead to low-frequency variability in SSTs in the equatorial Pacific via two processes. In the first, an influx of anomalous temperature, T', in the higher latitudes is injected into STCs. This occurs over the outcrop region of the isopycnals that constitute the equatorial thermocline. The anomalous temperature is then advected equatorward via the STCs into the source waters of the equatorial upwelling. Once these heat anomalies are upwelled into the surface in the tropics they affect the tropical and extratropical winds that in turn may affect the influx (hereafter referred to as the $\overline{V}T'$ process) of temperature anomalies in the outcrop regions of the higher latitudes. This can result in low-frequency self-sustaining oscillations (Gu and Philander, 1997; Zhang et al., 1998). However, observed temperature anomalies are weakened by mixing before reaching the equator (Nonaka and Xie, 2000), suggesting that the $\overline{V}T'$ process does not have a significant effect on equatorial SSTa.

In the second process, variations in the strength of the STC, V' alter the amount of cold water upwelled at the equator (the $V'\overline{T}$ process). Here, mean temperature properties in the outcrop region of the isopycnals are advected equatorward via the STCs. However, it is the variability of the strength of this transport (not the temperature) that leads to equatorial SSTa in the tropics and to the low-frequency oscillations (Kleeman et al., 1999).

McPhaden and Zhang (2002) analyzed 50 years of observational data that supported the process proposed by Kleeman et al. (1999). By examining the zonally-averaged transports at 9°N and 9°S, McPhaden and Zhang (2002) found that the meridional overturning circulation has been slowing since the 1970s, resulting in a decrease in equatorial upwelling. This reduction in the upwelling of relatively cool water is associated with a rise in equatorial SST of about 0.8°C and a reduction in the outgassing of CO_2 from the equatorial Pacific Ocean (McPhaden and Zhang, 2002).

Continuing with the $V'\overline{T}$ process, Nonaka et al. (2002) found that while on interannual time scales equatorial SSTa are driven by equatorial winds, on decadal time scales, they are driven by both equatorial and off-equatorial winds in the tropics. This is due to variability in the trade-winds that spin up and down the STCs, thereby altering the amount of cool water transported to the equatorial upwelling zone (Nonaka et al., 2002). The SSTa that result from this process lag the equatorial winds by about 2 years (Nonaka et al., 2002). Nonaka et al. (2002) also showed that wind variability poleward of 25° is unimportant for equatorial SSTa which was later supported by Capotondi et al. (2005). However, Capotondi et al. (2005) found that SSTa leads the interior meridional mass transport convergence across 9°N and 9°S by 2 months, which seems contrary to the view that changes in the strength of the STCs cause the SST variability.

1.3 Wind-Driven Ocean Gyres

Though changes in equatorial SST are linked to changes in the STCs, Hazeleger at al. (2004) discovered that total ocean heat transport may not be due solely to this meridional overturning circulation as horizontal wind-driven gyres also transport large amounts of heat toward the equator (e.g. Gordon et al., 2000). These large-scale gyres characterize the mean upper water circulation of the Pacific Ocean, both in the northern and southern hemispheres. The subtropical gyres are driven separately by trade winds in each hemisphere, rotating clockwise in the northern hemisphere and counterclockwise in the Southern, and are characterized by strong western boundary currents and relatively weak eastern boundary currents. The difference between the western and eastern boundary currents in the South Pacific is not as large as in the north because of the lack of a continuous boundary along the west and the exposure to the Southern Ocean which allows this gyre to be influenced by the Antarctic Circumpolar Current. A reduction in the trade winds decreases STC strength and causes the subtropical gyres to spin down (Hazeleger et al., 2004), further reducing heat transport toward the equator. Interaction between variability in the STCs and that of the gyre scale circulation on low frequencies may also play a role in equatorial SST.

Simonnet and Dijkstra (2002) found a significant mode of ocean variability, known as the 'gyre' mode by analyzing early bifurcations of ocean dynamics. A local bifurcation occurs when an equilibrium configuration transitions between stable and unstable states. Hopf bifurcations are local bifurcations between a steady state and a limit cycle. Bifurcation studies are useful in idealized models for determining the structure of steady states and large-scale instabilities (e.g. Cessi and Ierley, 1995; Jiang et al., 1995; Primeau, 1998; Nauw and Dijkstra, 2001; Simonnet and Dijkstra, 2002).

Nauw and Dijkstra (2001) used bifurcation analysis and trajectory computation to clarify the dynamical origin of low-frequency variability in a double gyre system using two-layer shallow-water equations with varying wind stress. They examined the

relationship between the sequence of Hopf bifurcations and low-frequency behavior. It was found that destabilization of asymmetric steady states are associated with low-frequency variability. Nauw and Dijkstra (2001) found a low-frequency mode in a double gyre system. Assuming flat-bottom topography, they showed that the modes of the first four Hopf bifurcations exhibit oscillation periods on the order of several months. However, the fifth Hopf bifurcation (higher wind stress) showed decadal oscillation. The inclusion of bottom topography revealed that less wind stress was needed to cause the decadal oscillation, appearing at even earlier bifurcations (Nauw and Dijkstra, 2001).

Berloff et al. (2007b) examined low-frequency gyre variability using a combination of long-term ocean-model integrations and the explicit representation of mesoscale eddies. It is important to dynamically resolve mesoscale eddies in ocean models because parameterizations of the mesoscale eddy effect by diffusion are not accurate (e.g. McIntyre, 1970; Berloff, 2005). They found large-scale flows are influenced by eddy-forcing fluctuations rather than time-mean eddy forcing; fluctuations in the eastward jet are dominated by isopycnal stretching rather than relative vorticity; and eddy forcing in the upper ocean dominates over eddy forcing in the deep (Berloff et al., 2007a). The low-frequency variability is driven by mesoscale eddies while the oceanic mode is driven by the opposition between the eddy rectification process and potential vorticity anomalies, which arise from changes in the inter-gyre transport barrier (Berloff et al., 2007b).

CHAPTER II

EXTERNAL DATA SETS AND METHODS

Monthly hindcast output from the Ocean General Circulation Model (OGCM) for the Earth Simulator (OFES; Masumoto et al., 2004; Sasaki et al., 2008) was used in this study. Based on the Modular Ocean Model (MOM3), the OFES domain is near global, covering the region extending from 75˚S to 75˚N with 0.1˚ spacing from 1950 to 2007. The spacing between the 54 vertical levels ranges from 5 meters at the surface to 330 meters at the bottom, enabling the reproduction of realistic ocean circulation above the main thermocline. Reanalysis data from the National Centers for Environmental Prediction-National Center for Atmospheric Research (NCEP/NCAR) (Kalnay et al., 1996) forces the surface wind stress, heat, and fresh water fluxes. This realistic output provides complete information in space and time as well as consistency between variations in wind forcing and ocean circulation while resolving mesoscale eddies.

2.1 Subtropical Cells

The strength of the STCs can be found by vertically and zonally integrating the anomalous velocities along different latitudes, while the heat transport can be similarly found by integrating the anomalous velocities times the mean temperature along different latitudes. There are different ways of choosing the latitudes along which to measure and at what depths to integrate.

Nonaka et al. (2002) measured the flow along 15°N and 11°S. These are the bifurcation latitudes for the North and South Equatorial Currents, where the currents diverge at the western boundary and flow either poleward to return to the subtropics or equatorward as part of the STCs (Nonaka et al., 2002). Since the flow is contained

between the ocean surface and 550m, Nonaka et al. (2002) integrated the meridional velocity along 15°N and 11°S between 0 and 550m.

McPhaden and Zhang (2002) chose 9°N to measure the flow in the North Pacific as this region is a choke point for meridional geostrophic transports in the interior. Since there is no such choke point in the South Pacific, they use 9°S for symmetry. To determine at which depths to integrate, McPhaden and Zhang (2002) noted that water less dense than 22 (sigma units) tends to fall within the surface mixed layer in the tropics, while water denser than 26 flows weakly poleward near the equator. Thus, their integration was done along 9°N and 9°S between isopycnals 22 and 26 (McPhaden and Zhang, 2002).

Capotondi et al. (2005) used a method similar to McPhaden and Zhang (2002) but chose slightly different depths for integration. Since the poleward Ekman transport along both latitudes is confined to the upper 50m of the ocean, they calculated the STC transport between 50m and isopycnal 26 along 9°N and 9°S.

The STC can be further divided into interior and boundary transports (McPhaden and Zhang, 2002). Variations in meridional velocity at the western boundary is anticorrelated with variations found in the interior because of the tendency for the boundary current to compensate for changes in the interior transport (e.g. Springer et al., 1990; Lee and Fukumori, 2003; Capotondi et al., 2005). Capotondi et al. (2005) found that changes in both interior and boundary currents are due to baroclinic adjustments of the ocean to large-scale wind stress curl variations.

Here, we use the OFES data to calculate both the strength of the STCs and the heat transport due to the STCs along 9°N and 9°S between 50 and the isopycnal 26. The latitudes chosen are just outside the boundaries of the subtropical gyres, while the depth range ensures the ability to encompass almost all of the mean STC without including the poleward Ekman transport. Additionally, we wish to consider only the interior transport, so the strength of the STCs is found by vertically integrating the meridional velocity

anomalies between the base of the Ekman layer (50m) to isopycnal 26 then zonally integrating between the eastern boundary and the edge of the western boundary currents (137°E at 9°N, 160°E at 9°S; Capotondi et al., 2005),

$$\text{STC strength} = \iint V' dx dz,$$

where V' is the anomalous meridional velocity.

In addition, we examine the heat transport due to variations in the STC. This is done by integrating the mean temperature times the meridional velocity anomalies in the regions described above,

$$\text{STC heat transport} = \rho_w \epsilon_p \iint V'\overline{T} dx dz,$$

where ρ_w is the density of seawater, c_p is the specific heat, V' is the anomalous meridional velocity, and $\overline{T}$ is the mean temperature. This is the $V'\overline{T}$ process described by Kleeman et al. (1999) and McPhaden and Zhang (2002). The heat transport is compared to the SSTa averaged within a region at the equator. This region, from 140°W to 90°W and 1°S to 1°N, is used because it exhibits large decadal SST variability (Nonaka et al., 2002).

2.2 Wind-Driven Ocean Gyres

The OFES output was again used to investigate the subtropical gyre system. This was done by computing a streamfunction along different isopycnals. Bernoulli's Law states that

$$\frac{1}{2}\rho v^2 + \rho g z + p = \text{constant},$$

where ρ is the density of the fluid, v is the velocity, g is gravity, z is depth, and p is pressure. Assuming the water is inviscid, has constant density along the streamline, and the streamline does not enter a boundary layer, an increase in the speed of the water results in a decrease in the pressure. Therefore, integrating the pressure of a column of

water above each point along an isopycnal produces the streamfunction which enables determination of the timescales of variability along that isopycnal.

The strength of the gyre can be computed as the gradient of the streamfunction along the edge of the gyre. Due to intensification of the western boundary currents, flow along the gyres is not symmetrical; therefore, it is important to examine the strength at various locations. In some cases, it is enough to place a box in the region of interest and compute the gradient within the box; however, it is not always possible to ensure that the gradient computed is entirely within the gyre as the position of the gyre can change drastically. In the worst case scenario, the gradient computed is entirely outside the boundary of the gyre. To solve this, the boundary was defined for the northern and southern subtropical gyres using a minimum value of the Bernoulli streamfunction in each gyre. This allows the gradient to be computed solely within the gyre along different sections of the boundary.

CHAPTER III

RESULTS

To examine the variability of the STCs we looked at both the strength of the STCs and their heat transport. Once again, the strength of the STCs is defined as the vertical and zonal integration of meridional velocity anomalies between the base of the Ekman layer (50m) to isopycnal 26 (sigma units) and between the eastern boundary and the edge of the western boundary currents along 9°N and 9°S; while the heat transport was found by integrating the mean temperature times the meridional velocity anomalies in the same regions.

The combined heat transport due to the STCs ($V'\overline{T}$) exhibits decadal variability as expected (Figure 1a, variances are normalized in all plots by dividing the signal by its standard deviation) and is highly correlated with equatorial SSTa (-0.80, greater than 99% significance) on low-frequencies. Low-frequency variability of the STCs is examined because this removes the shorter interannual time-scales associated ENSO dynamics. This was done by using discrete Fourier transforms to remove periods shorter than 8 years, specifically the ENSO band between 2-7 years. When the transport is separated into its northern and southern components, it becomes evident that the pattern of decadal variability in the southern branch alone is more correlated with the equatorial SSTa than the northern branch alone (Figure 1b,c). The correlation between the SSTa and the southern STC is -0.74, while with the northern STC is -0.61.

This is consistent with the streamfunction found along 165°W (Figure 2). In the South Pacific, one transport cell can be seen. This cell brings water to the equator that is subducted locally. In the North Pacific there are two transport cells near the tropics/subtropics. The first is confined between the equator and 5°N and is known as the

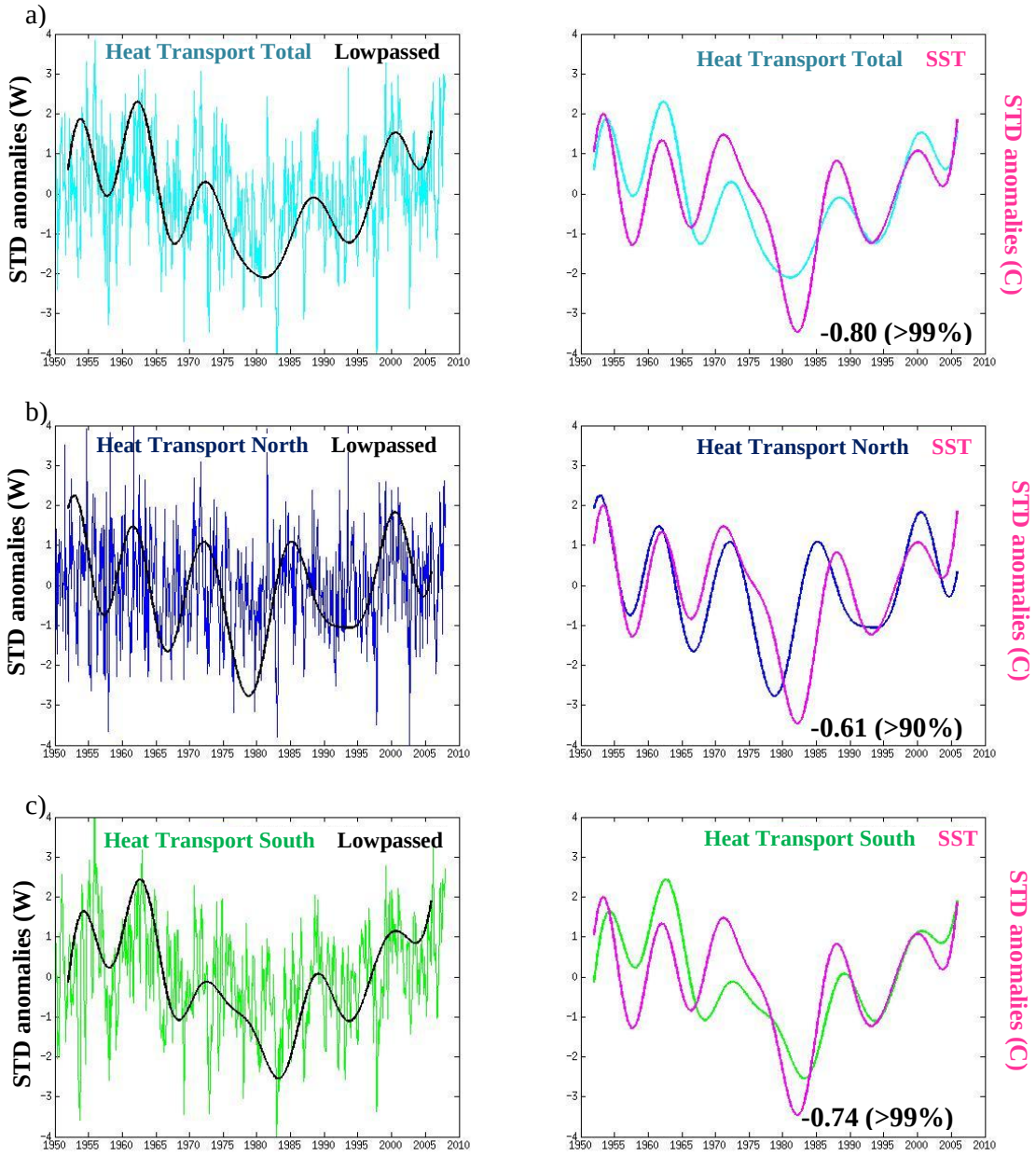

Figure 1. The left column shows heat transport due to the STCs where the black line is the decadal component found by removing frequencies shorter than 8 years. The right column shows the decadal components of the heat transport and equatorial SSTa (pink). The top panel (a) is the combined branches of the STCs (cyan), (b) is the northern branch alone (blue), and (c) is the southern branch (green). High correlations were found between the total heat transport and SSTa (a, -0.80 correlation) and the southern component of the heat transport and SSTa (c, -0.74 correlation). The correlation between the northern component of the heat transport and SSTa was significant only above the 90% threshold (b, -0.61 correlation). SSTa signs are reversed in these plots.

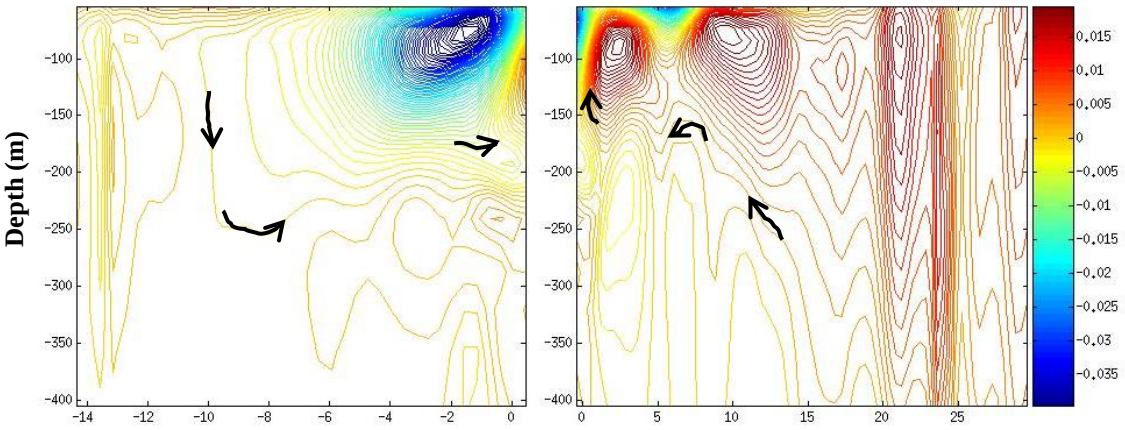

Figure 2. Meridional streamfunction along 165°W. The left box is of the South Pacific, right is the North Pacific, units are in Sverdrups. Arrows indicate the direction of water parcels following the STCs.

tropical cell (TC). The second (the STC) centers around 10°N. The majority of the water transported via this cell does not reach the equator with the exception of water below 170m. This water appears to have originated much further poleward than in the South Pacific. Overall, meridional transport in the South Pacific exhibits a clear and direct path to the equator, while transport in the North Pacific can lead to equatorial or off-equatorial upwelling.

Though the correlation between the heat transport of the northern STC and equatorial SSTa is not significant (>90% significance) and is low compared to the southern branch, the patterns of decadal variability match very well before the climate shift in the late 1970s. Figure 3 are plots of the heat transport versus equatorial SSTa on decadal timescales split into 2 periods, before and after the 1976/77 climate shift. Before the climate shift, the heat transport due to the northern branch of the STC is highly correlated (-0.89) with the SSTa while the southern branch is not. After the shift, the reverse is the case, with the southern branch correlating well (-0.85) with SSTa.

It has been found that the western boundary currents are anticorrelated with the interior (e.g. Spinger et al., 1990; Lee and Fukumori, 2003; Capotondi et al., 2005). When including all frequencies, the transports in the north and south are correlated with

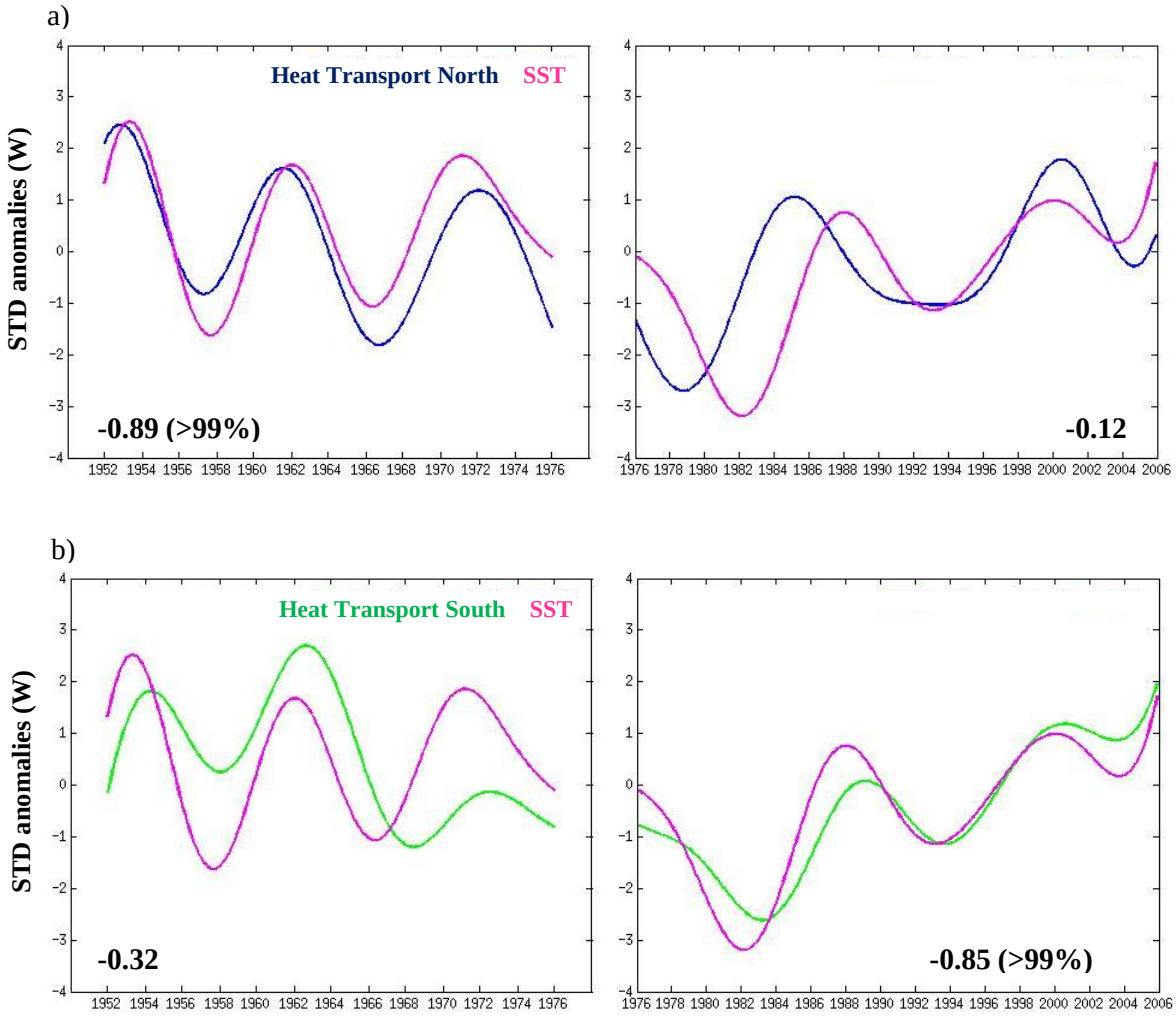

Figure 3. (a) and (b) show the decadal component of the STC heat transport in the northern and southern branches respectively with equatorial SSTa. The left panel is before 1976, while the right is after. Before 1976, the correlation in the northern branch is -0.89, in the southern branch is -0.32. After, the correlation in the north is -0.12 and in the south is -0.85.

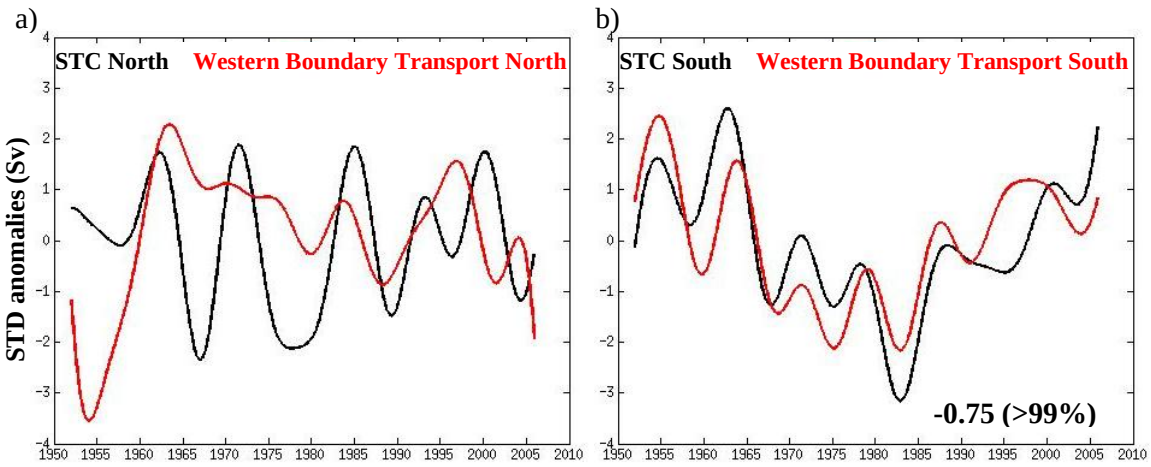

Figure 4. (a) shows the northern component of the STC (black) versus the western boundary transport (red) on decadal timescales. (b) is the same as (a) but for the southern components. Only the southern branch showed any correlation with the western boundary transport when lowpassed. Both the north and south were correlated well (>99%) with the western transport on high frequencies. Western boundary transport signs are reversed in both figures.

their western boundary counterparts (-0.59 in the north, -0.75 in the south). However, on decadal time scales a correlation was found only in the South Pacific (-0.75, Figure 4b). In the North Pacific, the STC is not correlated with its western boundary current on low frequencies (Figure 4a). The same appears to be the case with the local zonal wind stress. Figures 5a and 5c are correlation maps of the lowpassed STC versus the lowpassed zonal wind stress in the north and south respectively. The strong negative correlation between the southern STC and the wind along 9°S can be seen in Figure 5d. There was no significant correlation between the northern branch of the STC and the zonal wind stress (Figure 5a,b), though meridional transports computed poleward of the northern STC were correlated with the local wind stress on decadal timescales. However, the northern STC and local zonal wind stress do seem to be correlated before the climate shift. Separating the northern STC into the periods before and after the 1976 reveal the high correlation before (-0.73, >95%) and the lack of any correlation after (Figure 6).

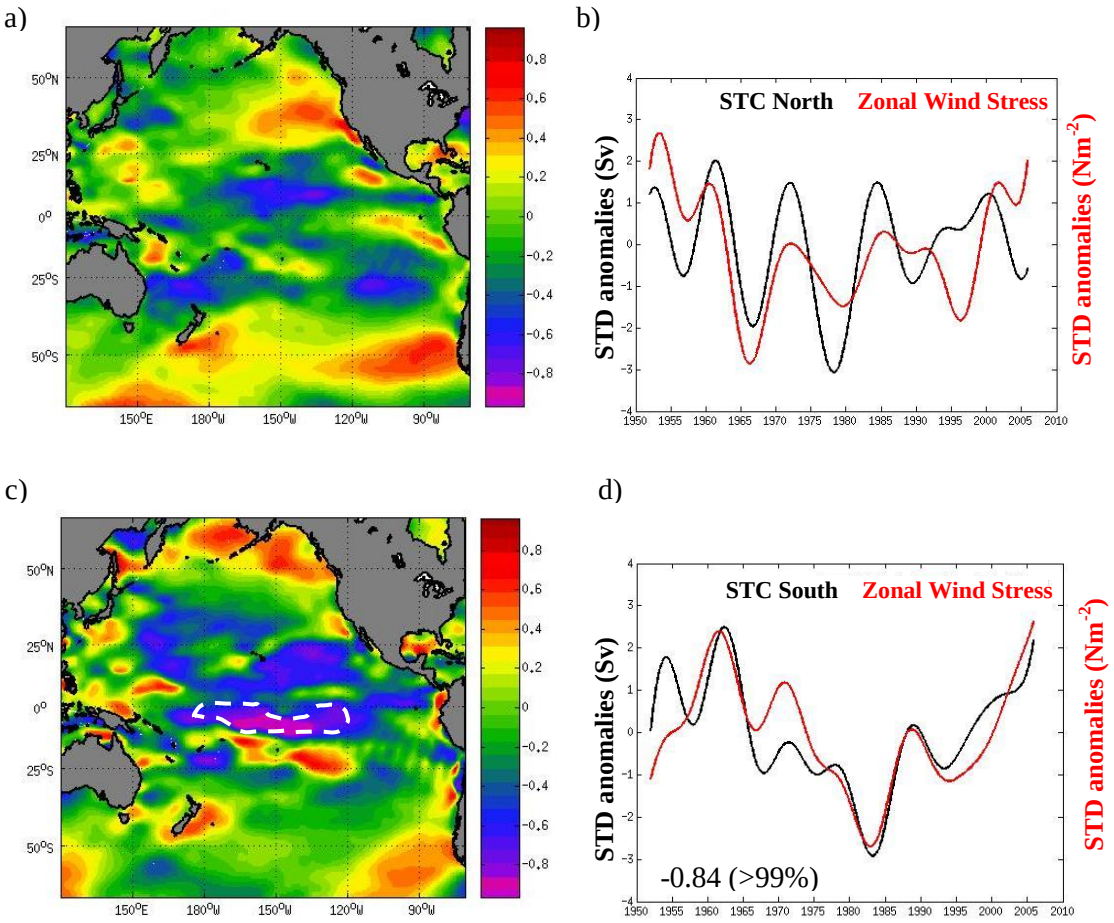

Figure 5. Correlation maps of the heat transport due to the STCs versus the zonal wind stress (Nm^{-2}). (a) and (b) are for the north, (c) and (d) for the south. The region outlined in (c) was found to be significant. None of the correlations found in (a) were significant above the 95% threshold. (b) and (d) are plots of the northern and southern STCs (black) versus the local zonal wind stress in each region (red).

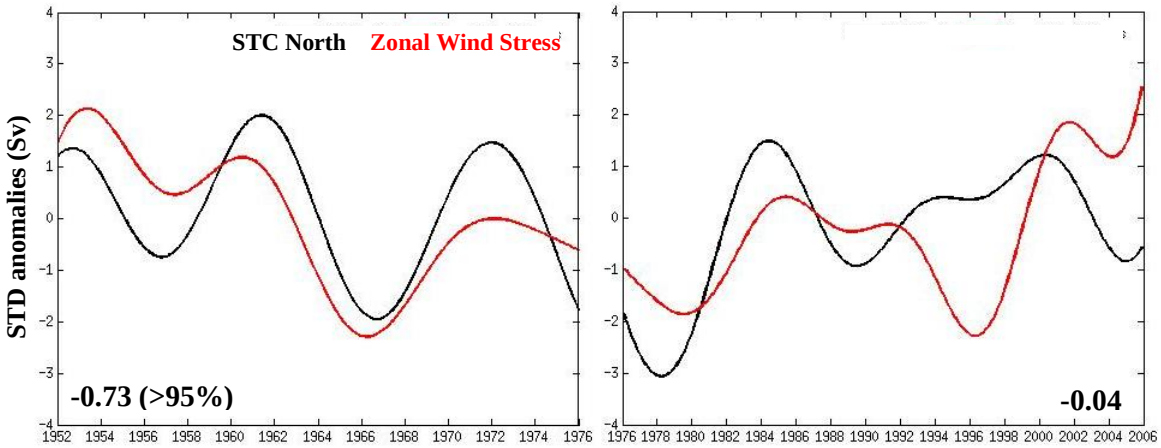

Figure 6. Decadal component of the STC in the North Pacific (black) and local zonal wind stress (red) is shown for the periods before and after 1976. Before, the 2 signals are well correlated (-0.73, >95%), while after there is no correlation.

To explore the relationship between the subtropical gyres and the STCs (V'), we computed the strength of the streamfunction along isopycnal 27.5. Because the strength of the gyres is the same with depth, we chose the isopycnal along which it is easiest to distinguish the boundaries of the gyres. The boundaries of the gyres are shown for multiple time steps in Figure 7a (boxes indicate regions where the gradient of the streamfunction was computed). The southern branch of the STC is highly correlated with the gradient in the northeastern part of the southern subtropical gyre (black box, -0.81 >99%, Figure 7b). This could be due to the proximity of the southern subtropical gyre to the STC.

Next we determine if there is any coherency among the subtropical gyres on decadal timescales. We find significant coherency occurs in the southern subtropical gyre but not in the northern gyre on low frequencies. Figure 8b shows a plot of the gradient in 3 regions of the gyre. These regions are outlined in Figure 8a. The blue box is the region that is best correlated with the heat transport of the southern branch of the STC. It is correlated positively with the region immediately adjacent to it (0.74) and negatively correlated with the region in the green box (-0.71). Both regions in the

northward flowing part of the gyre are correlated with each other (Figure 9a,b, 0.53 >95%). However, correlations could not be accurately determined around New Zealand because of the difficulty in computing the gradient there.

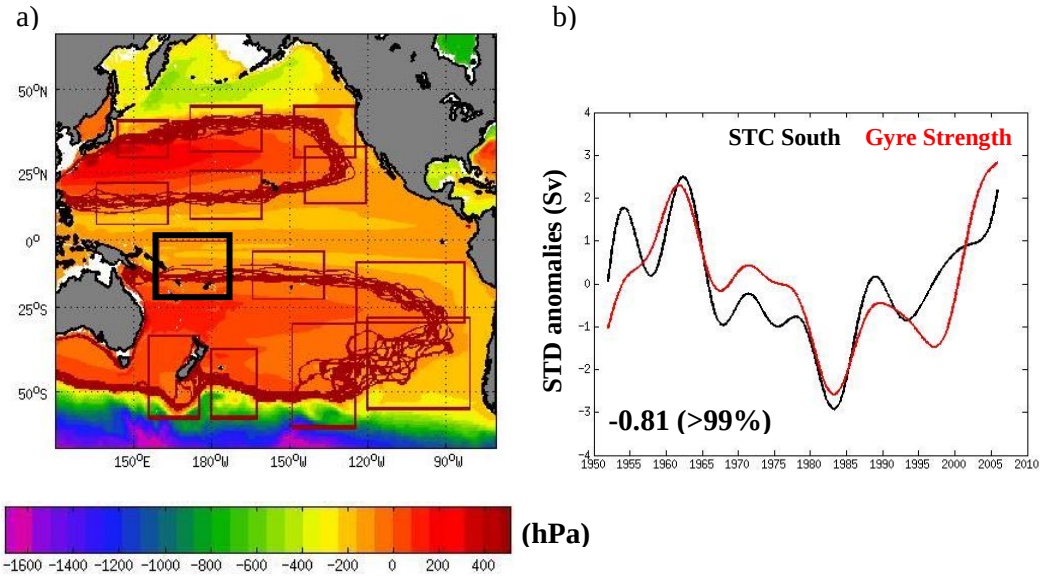

Figure 7. The streamfunction along isopycnal 27.5 and gyre boundaries computed at several time steps are shown in (a). Boxes indicate regions where the gradient was computed. (b) is a plot of the heat transport of the southern STC (black) and the strength of the subtropical gyre (red, reversed sign) computed within the black box in (a). A correlation of -0.81 was found (>99% significant).

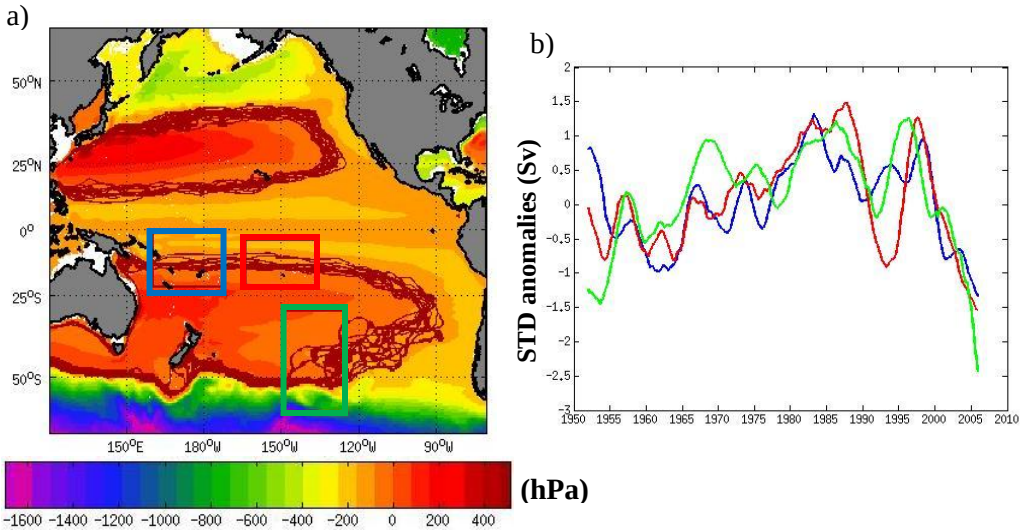

Figure 8. The streamfunction along isopycnal 27.5 and gyre boundaries computed at several time steps are shown in (a). The 3 boxes shown are well correlated with each other on low frequencies. (b) is a plot of the gradient found in each box (colors correspond to the boxes in a, the gradient in the green box is inverted). The correlation between the blue and red regions is 0.74 (99%), blue and green is -0.71 (99%), and red and green is -0.61 (95%).

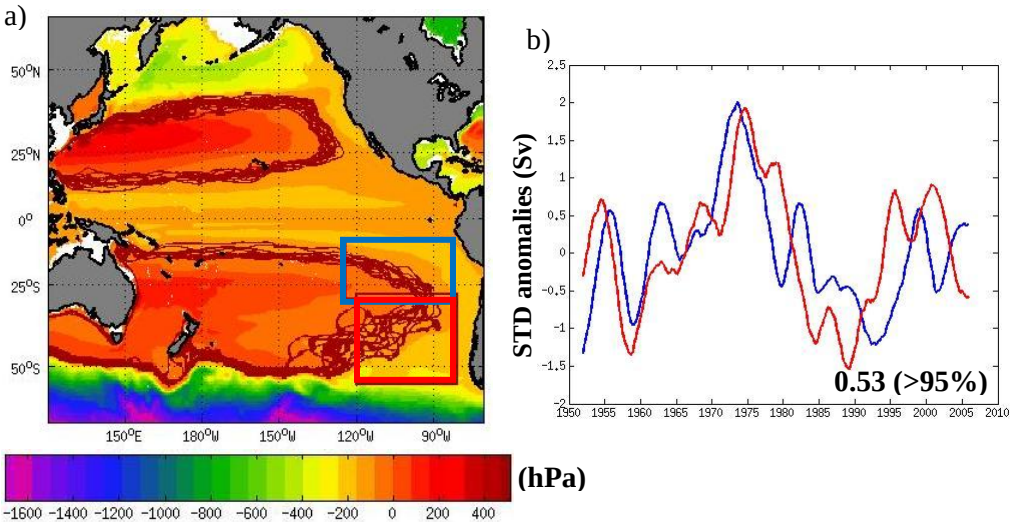

Figure 9. (a) is the same as in Figure 7a. The 2 boxes shown are well correlated with each other on low frequencies. (b) is a plot of the gradient found in each box (colors correspond to the boxes in a). The correlation found was 0.53 (above the 95% significance mark).

CHAPTER IV

SUMMARY AND CONCLUSIONS

The aim of this thesis is to investigate possible dynamical pathways through which variability in the extra-tropical Pacific Ocean influences low-frequency fluctuations of the sea surface temperatures in the tropical Pacific beyond ENSO timescales. Specifically, this work explored the relationship between variability in the meridional subtropical cells (STCs) of the Pacific Ocean and decadal modulation of the equatorial sea surface temperature anomalies (SSTa). We tested the hypothesis that low-frequency variations in the strength of the equatorward subsurface transport of the STCs in both the northern and southern hemisphere control temperature anomalies in the thermocline waters that are upwelled in the eastern and central tropical Pacific. This hypothesis is explored under the assumption that variations in the STCs on timescales longer than 8 years are controlled by atmospheric variability in the extra-tropical winds suggested to be independent of ENSO and tropical dynamics. This assumption is based on findings by previous studies and is critical because on the shorter interannual time-scales, changes in the trade winds associated with ENSO dynamics control the strength of the STCs through off equatorial Ekman dynamics (e.g. Nonaka et al., 2002).

The relationship between the STCs and equatorial Pacific SSTa was explored statistically using the monthly hindcast output from the Ocean General Circulation Model (OGCM) for the Earth Simulator (OFES). The strength of the STCs was defined as the vertical and zonal integration of meridional velocity anomalies between the base of the Ekman layer (50m) to isopycnal 26 and between the eastern boundary and the edge of the western boundary currents along 9°N and 9°S. The heat transport due to the STCs was found by integrating the mean temperature times the meridional velocity anomalies in the

same regions. The equatorial SST was found in the area from 140°W to 90°W and 1°S to 1°N.

Our results suggest that the decadal variability of the equatorward subsurface heat transport associated with the northern and southern hemisphere STCs is strongly correlated with equatorial SSTa (R = -0.80, >99%; Figure 1a) on timescales longer than 8 years. The southern branch of the STC is more closely correlated (R = -0.74, >99%; Figure 1c) with tropical SSTa, possibly due to the more direct path that its transport has to the equator (Figure 2). We also found that the southern branch of the STC is well correlated with the local zonal wind stress and the strength of the subtropical gyre (Figures 5, 7). The correlation pattern of the zonal wind stress with the southern STC has its maximum off the equator around 8°S, which may suggest that this forcing is independent of the equatorial dynamics. On the other hand, we noted that the correlation pattern exhibits some symmetry around the equator, which could be indicative of equatorial dynamics driving the winds. For the northern branch of the STC we find an overall lower and insignificant correlation with tropical SSTa (R = -0.61, > 90%; Figure 1b). This may be due to the more complex circulation structure in the subtropical North Pacific (Figure 2). The subsurface return flow of the northern branch of the STC does not have a direct path to the equator and part of the water is upwelled around 6°N. The water that upwells at the equator is mostly supplied by the tropical cell located between 0-4°N.

Although the overall correlation of the northern STC with tropical SSTa is not high, we found that in the period before the 1976 climate shift, the northern cell is strongly and significantly correlated with equatorial SSTa (R = -0.89, >99%; Figure 3a), while the southern cell is not (R = -0.32). On the other hand, after 1976 the southern STC exhibits stronger correlation (R = -0.85, >99%; Figure 3b) with equatorial SSTa than the northern STC (R = -0.12). This explains from a correlation standpoint why the combined effect of the two STCs explains more variance in the equatorial SSTa than the

individual components. From a dynamical standpoint, it suggests that both STCs play a role in modulating low-frequency fluctuations in the tropical temperatures. Given the low degrees of freedom in the correlations of the individual STC branches during the periods before and after 1976 and the lack of a mechanism that that could lead to an asymmetry in the role of the northern and southern STC, the significance of the changes before and after 1976 suggest an avenue for future research. In this regard, we also note that we were unable to isolate a clear physical mechanism that drives the northern STC. Isolating the forcing dynamics of the northern STC is critical in order to diagnose the impacts of the 1976 climate shift of the North Pacific.

Due to the lack of a clear physical forcing of the STC, we explored whether the low-frequency changes of the STC were connected to variations in the strength of the subsurface gyre-scale circulation of the Pacific. Interestingly, we found that fluctuations of the subtropical gyre's strength on timescales longer than the Rossby wave adjustment period (>8 years in the extra-tropics) are not coherent and are uncorrelated with the STC except in the region close to the western boundary return flow. This is in contrast to work by Hazeleger et al. (2004) that found a relationship between the gyre spin-down and trade winds. However, they use a coarse resolution model with 2.5˚ spacing while the OFES high resolution model has 0.1˚ spacing. Although this result does not provide us with additional interpretive frameworks for the forcing dynamics of the STC, it does raise an interesting question regarding the low-frequency dynamics of the subtropical gyres of the Pacific, with may be explored in future studies.

REFERENCES

Berloff, P., W. Dewar, et al., "Ocean eddy dynamics in a coupled ocean - Atmosphere model," *Journal of Physical Oceanography, 37*, 1103-1121, 2007a.

Berloff, P., A. M. Hogg, et al., "The turbulent oscillator: A mechanism of low-frequency variability of the wind-driven ocean gyres," *Journal of Physical Oceanography, 37*, 2363-2386, 2007b.

Berloff, P. S., "On dynamically consistent eddy fluxes," *Dynamics of Atmospheres and Oceans, 38,* 123-146, 2005.

Capotondi, A., M. A. Alexander, et al., "Anatomy and decadal evolution of the Pacific Subtropical-Tropical Cells (STCs)," *Journal of Climate 18,* 3739-3758, 2005.

Cessi, P. and G. R. Ierley, "Symmetry-breaking multiple equilibria in quasi-geostrophic, wind-driven flows," *Journal of Physical Oceanography, 25*, 1196–1205, 1995.

Colin de Verdière, A. and T. Huck, "Baroclinic Instability: An Oceanic Wavemaker for Interdecadal Variability," *Journal of Physical Oceanography, 29*, 893-910, 199.

Chhak, K. C., E. Di Lorenzo, et al., "Forcing of Low-Frequency Ocean Variability in the Northeast Pacific," *Journal of Climate 22,* 1255-1276, 2009.

Delworth, T. L., "North Atlantic interannual variability in a coupled ocean-atmosphere model," *Journal of Climate, 9*, 2356-2375, 1996.

Deser, C., A.S. Phillips, J.W. Hurrell, "Pacific interdecadal climate variability: Linkages between the tropics and North Pacific during boreal winter," *Journal of Climate, 17*, 3109-3124, 2004.

Di Lorenzo, E., N. Schneider, et al., "North Pacific Gyre Oscillation links ocean climate and ecosystem change," *Geophysical Research Letters, 35*, 2008.

Di Lorenzo, E., N. Schneider, et al., "ENSO and the North Pacific Gyre Oscillation: an intergrated view of Pacific decadal dynamis," *Geophysical Research Letters, submitted,* 2009.

Enfield, D. B. and J. S. Allen, "On the Structure and Dynamics of Monthly Mean Sea Level Anomalies along the Pacific Coast of North and South America," *Journal of Physical Oceanography, 10,* 557-578, 1980.

Folland, C. K., J. A. Renwick, M.J. Salinger, and A. B. Mullan, "Relative influences of the Interdecadal Pacific Oscillation and ENSO on the South Pacific Convergence Zone," *Geophysical Research Letters, 29,* 2002.

Gordon, C., C. Cooper, et al., "The simulation of SST, sea ice extents and ocean heat transports in a version of the Hadley Centre coupled model without flux adjustments," *Climate Dynamics, 16,* 147-168, 2000.

Graham, N. E., "Decadal-scale climate variability in the tropical and North Pacific during the 1970s and 1980s: observations and model results," *Climate Dynamics, 10,* 135-62, 1994.

Gu, D. F. and S. G. H. Philander, "Interdecadal climate fluctuations that depend on exchanges between the tropics and extratropics," *Science, 275,* 805-807, 1997.

Hare, S. R., et al., "Inverse production regimes: Alaska and West Coast Pacific salmon" *Fisheries, 24,* 6-14, 1999.

Hazeleger, W., R. Seager, et al., "How can tropical Pacific Ocean heat transport vary?" *Journal of Physical Oceanography, 34,* 320-333, 2004.

Horel, J. D, and J. M. Wallace, "Planetary-scale atmospheric phenomena associated with the Southern Oscillation," *Monthly Weather Review, 109,* 813-829 1981.

Huck, T., A. C. de Verdière, et al., "Interdecadal variability of the thermohaline circulation in box-ocean models forced by fixed surface fluxes," *Journal of Physical Oceanography, 29,* 865-892, 1999.

Jiang, S., F.-F. Jin, and M. Ghil, "Multiple equilibria and aperiodic solutions in a wind-driven double gyre, shallow water model," *Journal of Physical Oceanography, 25,* 764–786, 1995.

Kalnay, E., M. Kanamitsu, et al., "The NCEP/NCAR 40-year reanalysis project," *Bulletin of the American Meteorological Society, 77, 437*-471, 1996.

Kleeman, R., R. Colman, N.R. Smith, and S.B. Power, "A recent change in the mean state of the Pacific basin climate: Observational evidence and atmospheric and ocean responses," *Journal of Geophysical Research, 101,* 20,483-20,499, 1996.

Kleeman, R., J. P. McCreary, et al., "A mechanism for generating ENSO decadal variability," *Geophysical Research Letters, 26,* 1743-1746, 1999.

Latif, M. and T. P. Barnett, "Causes of Decadal Climate Variability over the North Pacific and North-America," *Science 266,* 634-637, 1994.

Latif, M. and T. P. Barnett, "Decadal climate variability over the North Pacific and North America: Dynamics and predictability," *Journal of Climate, 9,* 2407-2423, 1996.

Latif, M., R. Kleeman, and C. Eckert, "Greenhouse warming, decadal variability or El Niño? An attempt to understand the anomalous 1990s," *Journal of Climate, 8,* 2221-2239, 1997.

Lee, T., and I. Fukumori, "Interannual-to-decadal variations of tropical-subtropical exchange in the Pacific Ocean: Boundary versus interior pycnocline transports," *Journal of Climate, 16,* 4022–4042, 2003.

Linkin, M. E. and S. Nigam, "The north pacific oscillation-west Pacific teleconnections pattern: Mature-phase structure and winter impacts," *Journal of Climate, 21,* 1979–1997, 2008.

Liu, Z., "A simple model of the mass exchange between the subtropical and tropical ocean," *Journal of Physical Oceanography, 24,* 1153–1165, 1994.

Luyten, J. R., J. Pedlosky, et al., "The Ventilated Thermocline," *Journal of Physical Oceanography, 13,* 292-309, 1983.

Lysne, J., P. Chang, et al., "Impact of the extratropical Pacific on equatorial variability," *Geophysical Research Letters, 24,* 2589-2592, 1997.

Mantua, N. J., S. R. Hare, et al., "A Pacific interdecadal climate oscillation with impacts on salmon production," *Bulletin of the American Meteorological Society, 78,* 1069-1079, 1997.

Masumoto, Y., and Coauthors, "A fifty-year eddy-resolving simulation of the World Ocean - preliminary outcomes of the OFES (OGCM for the Earth Simulator)," *Journal of the Earth Simulator, 1,* 35-56, 2004.

McCreary, J. P., and P. Lu, "Interaction between the subtropical and equatorial ocean circulations: The subtropical cell," *Journal of Physical Oceanography, 24,* 466–497, 1994.

McIntyre, M., "On the non-separable baroclinic parallel flow instability problem," *Journal of Fluid Mechanics, 40,* 273–306, 1970.

McPhaden, M. J., and D. Zhang, "Decadal Spin-down of the Pacific Ocean Shallow Meridional Overturning Circulation," *Nature, 415,* 603-608, 2002.

Miller, A. J., D. R. Cayan, et al., "Interdecadal Variability of the Pacific-Ocean - Model Response to Observed Heat-Flux and Wind Stress Anomalies," *Climate Dynamics, 9,* 287-302, 1994.

Nauw, J. J. and H. A. Dijkstra, "The origin of low-frequency variability of double-gyre wind-driven flows," *Journal of Marine Research, 59,* 567-597, 2001.

Nitta, T. and S. Yamada, "Recent Warming of Tropical Sea-Surface Temperature and Its Relationship to the Northern Hemisphere Circulation," *Journal of the Meteorological Society of Japan, 67,* 375-383, 1989.

Nonaka, M., and S.-P. Xie, "Propagation of North Pacific interdecadal subsurface temperature anomalies in an ocean GCM," *Geophysical Research Letters, 27,* 3747– 3750, 2000.

Nonaka, M., S. P. Xie, et al., "Decadal variations in the subtropical cells and equatorial pacific SST," *Geophysical Research Letters, 29,* 2002.

Philander, S. G. H., "El-Nino Southern Oscillation Phenomena," *Nature, 302,* 295-301, 1983.

Pierce, D. W., T. P. Barnett, et al., "Connections between the Pacific Ocean tropics and midlatitudes on decadal timescales," *Journal of Climate, 13,* 1173-1194, 2000.

Power, S., T. Casey, C. K. Folland, A. Colman, and V. Mehta, "Inter-decadal modulation of the impact of ENSO on Australia," *Climate Dynamics, 15,* 319-323, 1999.

Primeau, F. W., "Multiple equilibria of a double-gyre ocean model with super-slip boundary conditions," *Journal of Physical Oceanography, 28,* 2130–2147, 1998.

Rogers, J. C., "The North Pacific Oscillation," *Journal of Climate, 20,* 3602-3620, 1981.

Sasaki, H., M. Nonaka, Y. Masumoto, Y. Sasai, H. Uehara, and H. Sakuma, "An eddy-resolving hindcast simulation of the quasiglobal ocean from 1950 to 2003 on the Earth Simulator," High Resolution Numerical Modeling of the Atmosphere and Ocean, K. Hamilton and W. Ohfuchi, Eds., Springer New York, 157–185, 2008.

Schneider, N. and B. D. Cornuelle, "The forcing of the Pacific decadal oscillation," *Journal of Climate, 18,* 4355-4373, 2005.

Simonnet, E. and A. Dijkstra, "Spontaneous Generation of Low-Frequency Modes of Variability in the Wind-Driven Ocean Circulation," *Journal of Physical Oceanography, 32,* 1747-1762, 2002.

Solomon, A., J. P. McCreary Jr., R. Kleeman, and B. A. Klinger, "Interannual and decadal variability in an intermediate coupled model of the Pacific region," *Journal of Climate, 16,* 383–405, 2003.

Springer, S. R., M. J. McPhaden, and A. J. Busalacchi, "Oceanic heat content variability in the tropical pacific during the 1982-1983 El Niño," *Journal of Geophysical Research, 95,* 22 089-22 101, 1990.

Stommel, H., "Determination of Water Mass Properties of Water Pumped down from the Ekman Layer to the Geostrophic Flow Below," *Proceedings of the National Academy of Sciences of the United States of America, 76,* 3051-3055, 1979.

Te Raa, L. and H. A. Dijkstra, "Instability of the Thermohaline Ocean Circulation on Interdecadal Timescales," *Journal of Physical Oceanography, 32,* 138-160, 2001.

Trenberth, K. E. and J. W. Hurrell, "Decadal atmosphere - ocean variations in the Pacific," *Climate Dynamics, 9,* 303-319, 1994.

van Loon, H. and R. A. Madden, "The Southern Oscillation: Part I: Global associations with pressure and temperature in northern winter," *Monthly Weather Review, 109,* 1150-1162, 1981.

Walker, G., "World Weather," *Monthly Weather Review, 56,*167-170, 1928.

Walker, G. and E. Bliss, "World weather V," *Memoirs of the Royal Meteorological Society, 4,* 53-85, 1932.

Wang, X. L. and C. F. Ropelewski, "An assessment of ENSO-scale secular variability," *Journal of Climate, 8,* 1584–1589, 1995.

Wyrtki, K., "El Niño - Dynamic-Response of Equatorial Pacific Ocean to Atmospheric Forcing," *Journal of Physical Oceanography, 5,* 572-584, 1975.

Zhang, R.-H., L. M. Rothstein, and A. J. Busalacchi, "Origin of warming and El Niño change on decadal scales in the tropical Pacific Ocean," *Nature, 391,* 879–883, 1998.